An AC/DC Power Conversion Based on Series-connected Universal Link Converter

Anno Yoo, Student member
Myoungho Kim, Student Member
and Seung-Ki Sul, Fellow

Seoul National University
School of Electrical Engineering & Computer Science #24, ENG-420, Seoul National University Gwanak P.O.BOX34, Seoul Korea (ZIP 151-744)
realanno@eepel.snu.ac.kr

***Abstract* -- This paper presents a novel AC/DC power converter topology for the future energy conversion network. The proposed Series-connected Universal Link (SUL) converter transfers the power via the high frequency transformers and single phase full bridge converters. The shape of input AC source current is sinusoidal without PWM switching of the input side converter. Thanks to the reduced reactive components and high frequency transformer, the proposed converter can increase the power density and the efficiency significantly. It is expected that the SUL converter can be easily adapted to various renewable energy sources and energy storage system. Experimental results with prototype show the effectiveness of the proposed power converter topology.**

***Index Terms*— AC/DC Series-connected Universal Link converter, bi-directional power flow, high frequency transformer, phase-shift control, sinusoidal input current.**

I. INTRODUCTION

In past, the energy is produced and consumed in uni-direction. That is, only large power plants can generate the electric power and the generated electric power is transmitted and distributed to the customers. However, the characteristics of the future energy network can be described as a bi-directional energy flow between the renewable energy sources and conventional utilities through Smart-Grid [1]. Because of the nature of renewable energy source, namely distributed and uncontrollable, the sources cannot be integrated to the conventional grid easily. Recently, due to the great concern about global warming, the integration of the large renewable energy source to the grid is imminent.

Still, the renewable sources are connected to the grid via power converters such as PWM boost rectifiers [2]-[4]. The grid-connected PWM boost rectifier needs the line frequency transformers, the large inductors and the bulky electrolytic capacitor in the DC-link. These huge reactive components sometimes limit the reliability and increase the total volume and maintenance cost.

There were several researches to reduce the capacitance in DC-link [5]-[8]. In [5] and [6], the PWM boost converter with reduced energy storage in DC-link was presented. Although its input current is sinusoidal, the capacitance of DC-link is dependent on the load power and the performance was sensitive to the parameter variation. In [7] and [8], an electrolytic capacitor-less inverter was proposed. Although the DC-link capacitance of electrolytic capacitor-less inverter was independent on the load power, the DC-link voltage has inevitable fluctuation according to the input voltage. Furthermore, the input current is quasi-square wave, and it cannot be connected to the grid directly where power quality is a concern. Also, it is still inevitable to install the line frequency transformer for galvanic isolation and flexibility of the voltage.

Ref. [9] shows an example of the power conversion based on the high frequency transformer, and many papers have been presented about the high-frequency power conversion system such as shown in [10]-[11]. In all papers, the power density can be enhanced conspicuously by employing a small high frequency transformer and it can provide the galvanic isolation and voltage flexibility. However, most of papers concentrated on bi-directional high frequency power conversion itself, and the grid-connection between the energy source and the grid was achieved by the PWM boost converter which has the bulk inductor and capacitor.

In this paper, a novel power converter topology to accommodate variable voltage DC source/load to the grid without the huge line frequency transformer and bulky reactive components is proposed. The DC source may come from the large solar panel or from wind power generators. Instead of the line frequency transformer, high frequency transformer can provide galvanic isolation and flexibility of the voltage to the system. The secondary windings of three high frequency transformers in the topology are connected in series to balance the instantaneous power of input AC source. With this series connection, the waveform of AC source current can be kept as sinusoidal and its power factor is controllable. Also, the proposed power converter utilizes the small film capacitor in DC-link instead of bulky electrolytic capacitor. With the reduced size of transformer and small film capacitor in DC-link, the proposed converter can improve the power density conspicuously. Because of the series connection of the secondary windings and also

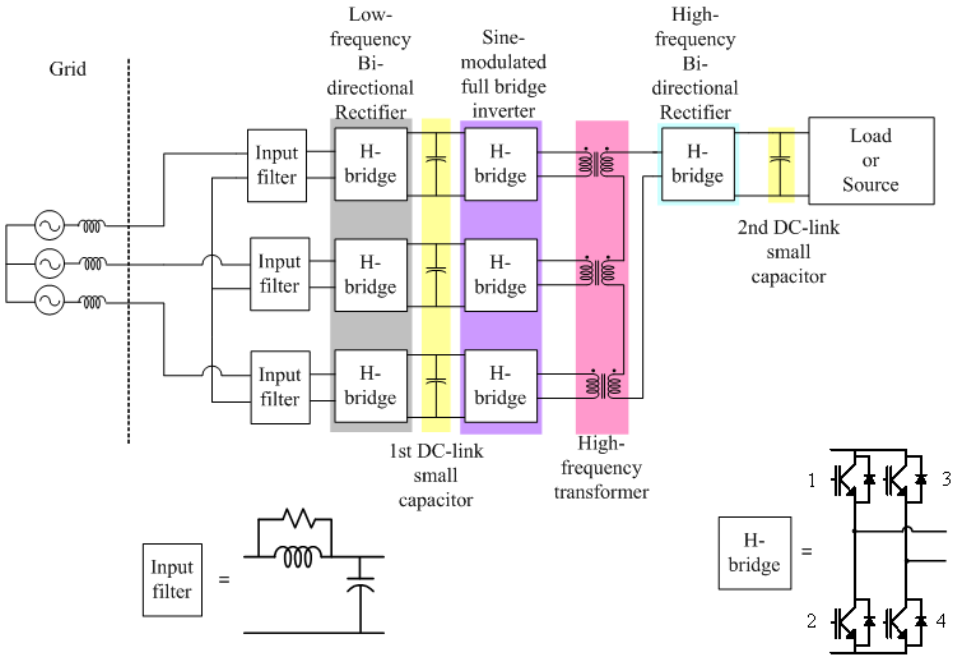

Fig. 1. Circuit diagram of proposed series-connected universal link AC/DC converter

possibility of the series connection of the converter itself to accommodate various AC/DC load/source at different voltage universally, the topology may be called as Series-connected Universal Link (SUL) converter. Some experimental results with a primitive prototype set are given to demonstrate the feasibility of SUL converter.

II. Proposed Series-connected Universal Link AC/DC Converter

A. Characteristics of SUL converter

Fig. 1 shows the circuit diagram of proposed SUL AC/DC converter. As shown, the proposed power converter is consisted of input filter, low-frequency bi-directional rectifier, 1st small capacitor, sine-modulated full bridge inverter, high-frequency transformer, high-frequency bi-directional rectifier, and 2nd small capacitor.

As shown, the proposed SUL converter is based on the input phase voltage and all switching components are in H-bridges. The capacity of low-frequency bi-directional rectifiers and sine-modulated full bridge inverters is same and that of high-frequency bi-directional rectifier is three times of capacity of the sine-modulated full bridge inverter. Also, the output voltages of sine-modulated full bridge inverters are connected in series through the high-frequency transformers

The bi-directional power flow can be achieved through the low frequency bi-directional rectifier and high frequency power conversion. In order to achieve the high frequency power conversion with consideration of the existing power semiconductors, the switching frequency of sine-modulated full bridge inverter and high-frequency bi-directional rectifier is set around ten kHz. Because of the high frequency operation, the size of transformer can be shrunken remarkably. Although there are three transformers in SUL converter, the total weight and volume of transformers are less than 1/20 of the line frequency transformer at the same power level.

The active switches in high-frequency bi-directional rectifier are operating in soft switching manner. Also, some of those in sine-modulated full bridge inverter are operating in soft switching manner too. Those in the low frequency bi-directional rectifier only switch synchronously with the anti-parallel diode to the switch, and its switching frequency is the input line frequency.

Because of small capacitance at 1st DC-link to decouple the stray inductance of DC-link, 1st DC-link voltage is the rectified version of the input AC phase voltage. Owing to the small capacitance in DC-link, the input AC current can be controlled as sinusoidal one. The capacitance of 2nd DC-link can be determined with consideration of the switching frequency of high-frequency power conversion and the demanded power level. As the switching frequency is increased, the capacitance of 2nd DC-link can be reduced under the same load condition.

Because the proposed power converter has small capacitance in 1st DC-link, the switching ripples of sine-modulated full bridge inverter can be transferred directly to grid side. In order to keep the switching ripple current from flowing into the grid, some input filters may be installed between AC source and SUL converter. In this paper, L-C

filter with damping resistor is used as an input filter and the cut-off frequency of the input filter is set as several kHz, and its size is kept as small as possible.

The sine-modulated full bridge inverter synthesizes the output voltage with the variable DC-link, and the output voltages of the inverter are connected in series through the high frequency transformers and the galvanic isolation can be achieved through the high frequency transformer. Owing to sine-modulation and series connection, the synthesized output voltage after the high-frequency bi-directional rectifier is constant on the average sense in a switching period.

Finally, the demanded power can be transferred with the phase-shift control between the series-connected output voltage of sine-modulated full bridge inverters and the output voltage of high frequency bi-directional rectifier. The power factor of grid side can be adjusted by the output voltage modification of sine-modulated full bridge inverter.

B. *Low frequency bi-directional rectifier*

The switch of low-frequency bi-directional rectifier connected to the grid turns on when their corresponding anti-parallel diode turns on. Fig. 2 shows the switching instant of low-frequency bi-directional rectifier according to the input phase voltages. In Fig.2, 'a', 'b', and 'c' means the input phase. As shown, the switching frequency of low-frequency bi-directional rectifier is equal to the grid frequency.

If the input phase voltage can be defined as (1), DC-link voltages of the input-side, namely 1st DC link, become absolute value of input phase voltage due to the small capacitance as described in (2).

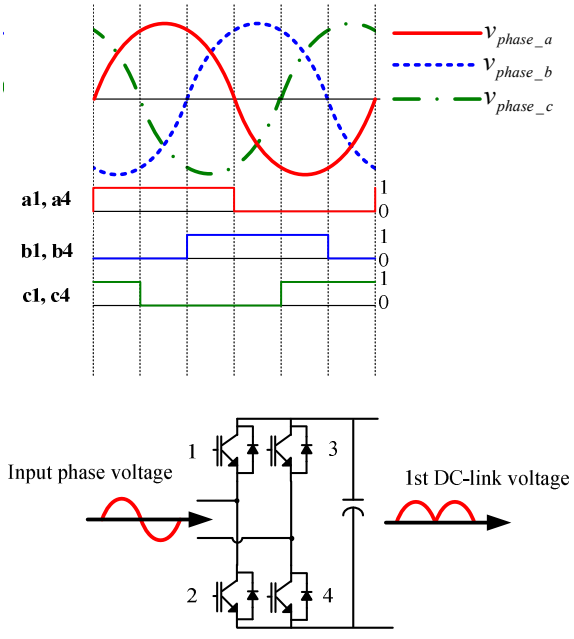

Fig. 2. Switching instance of low-frequency bi-directional rectifier and input 'a' phase voltages and DC-link voltage

$$\begin{aligned} V_{phase\_a} &= V\sin(\omega t) \\ V_{phase\_b} &= V\sin\left(\omega t - \frac{2}{3}\pi\right) \\ V_{phase\_c} &= V\sin\left(\omega t + \frac{2}{3}\pi\right) \end{aligned} \quad (1)$$

$$\begin{aligned} V_{dc\_a} &= V\left|\sin(\omega t)\right| \\ V_{dc\_b} &= V\left|\sin\left(\omega t - \frac{2}{3}\pi\right)\right| \\ V_{dc\_c} &= V\left|\sin\left(\omega t + \frac{2}{3}\pi\right)\right| \end{aligned} \quad (2)$$

C. *Sine-modulated full bridge inverters*

Using the 1st DC-link voltage of (2), the each output of sine-modulated full bridge inverter can be synthesized as (3) respectively.

$$\begin{aligned} V_{ac\_a} &= mV\left|\sin(\omega t)\right|\sin(\omega t)\,square(t) \\ V_{ac\_b} &= mV\left|\sin\left(\omega t - \frac{2}{3}\pi\right)\right|\sin\left(\omega t - \frac{2}{3}\pi\right)\,square(t) \\ V_{ac\_c} &= mV\left|\sin\left(\omega t + \frac{2}{3}\pi\right)\right|\sin\left(\omega t + \frac{2}{3}\pi\right)\,square(t) \end{aligned} \quad (3)$$

where '*square(t)*' is the square function whose peak to peak magnitude is 2 with no DC component, and '*m*' is the modulation index $(0 \le m \le 1)$. The frequency of the square wave is f_c, which is the switching frequency of all sine-modulated inverters . The switching frequency is much larger than the grid frequency.

Fig. 3 demonstrates the voltage synthesizing sequence of 'a' phase sine-modulated full bridge inverter.

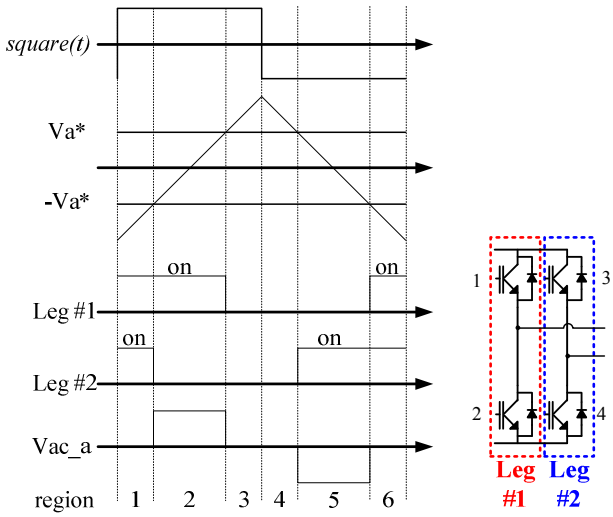

Fig. 3. Example of voltage synthesize of 'a' phase sine-modulated full inverter

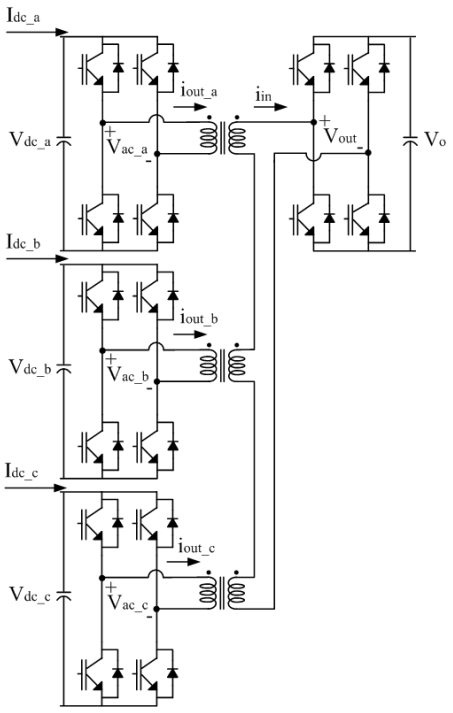

Fig. 4. Circuit diagram of sine-modulated full bridge inverters and high-frequency bi-directional rectifier

In Fig.3, 'Leg #1' is the left side leg of H-bridge and 'Leg #2' is right side of that. The frequency of triangular carrier is f_c and '*square(t)*' is '1' at rising instant of triangular carrier and '-1' at falling. The voltage reference of 'Leg #1' is 'V_a^*' when '*square(t)*' is '1' and it is '$-V_a^*$' when '*square(t)*' is '-1'. Also, it is vice verse in case of 'Leg #2'. Therefore, the synthesized voltage, 'V_{ac_a}', is positive value at the center of rising duration of triangular carrier and it is negative at the center of falling duration.

If the output voltages of sine-modulated full bridge inverters are series-connected through the high frequency transformer and the turn ratio of high frequency transformer is given as 1 : n, the series-connected output voltage can be derived as follows,

$$\begin{aligned} V_{syn\_sum} &= n\left(V_{ac\_a} + V_{ac\_b} + V_{ac\_c}\right) \\ &= \frac{3}{2} nmV\ square(t) \end{aligned} . \quad (4)$$

The magnitude of the series-connected output voltage is constant in the average sense of a switching period. Also, if the turn ratio of the high frequency transformer is set to 1.5:1, the magnitude of synthesized output voltage is equal to input phase voltage in average sense at a switching period and the all H-bridge modules can have the same voltage rating.

Fig. 4 shows the circuit diagram of sine-modulated full bridge inverters and the high-frequency bi-directional rectifier. As the outputs of sine-modulated full bridge inverter are series connected, the output currents of sine-modulated full bridge inverter and the input current of high-frequency bi-directional rectifier can be deduced as follows,

$$i_{in} = \frac{1}{n} i_{out\_a} = \frac{1}{n} i_{out\_b} = \frac{1}{n} i_{out\_c} . \quad (5)$$

If the modulation index, *m*, is '1' and the phase difference between the output voltage and current of sine-modulated full bridge inverter is small, the power balance equations can be derived at 1st DC-link as follows,

$$\begin{aligned} & V\left|\sin(\omega t)\right|\left|\sin(\omega t)\right| i_{out\_a} square^2(t) \\ &= V\left|\sin(\omega t)\right| I_{dc\_a} \\ & V\left|\sin\left(\omega t - \frac{2}{3}\pi\right)\right|\left|\sin\left(\omega t - \frac{2}{3}\pi\right)\right| i_{out\_b} square^2(t) \\ &= V\left|\sin\left(\omega t - \frac{2}{3}\pi\right)\right| I_{dc\_b} \\ & V\left|\sin\left(\omega t + \frac{2}{3}\pi\right)\right|\left|\sin\left(\omega t + \frac{2}{3}\pi\right)\right| i_{out\_c} square^2(t) \\ &= V\left|\sin\left(\omega t + \frac{2}{3}\pi\right)\right| I_{dc\_c} \end{aligned} . \quad (6)$$

Also, considering the switching function of the low-frequency bi-directional rectifier, the input phase currents can be represented as follows,

$$\begin{aligned} i_a &= sign\left(\sin(\omega t)\right) I_{dc\_a} = i_{out\_a} \sin(\omega t) \\ i_b &= sign\left(\sin\left(\omega t - \frac{2}{3}\pi\right)\right) I_{dc\_b} = i_{out\_b} \sin\left(\omega t - \frac{2}{3}\pi\right) \\ i_c &= sign\left(\sin\left(\omega t - \frac{2}{3}\pi\right)\right) I_{dc\_c} = i_{out\_c} \sin\left(\omega t + \frac{2}{3}\pi\right) \end{aligned} \quad (7)$$

where '*sign(x)*' is the sign function whose output is 1 at positive '*x*' and -1 at negative '*x*'.

By (5) and (7), the input currents of proposed power converter can be kept as sinusoidal and the magnitude of each phase is the same.

D. High-frequency power transfer

The high-frequency power transfer of the proposed converter can be achieved by phase-shift control between the series-connected sine-modulated full bridge inverter and high-frequency bi-directional rectifier. Fig. 5 depicts the model of high frequency power transfer of proposed converter at the switching frequency, f_c.

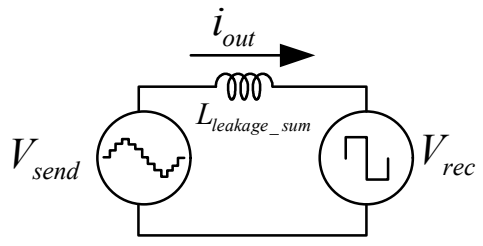

Fig. 5. A model of high frequency power transfer at f_c

In Fig.5, 'V_{send}' is the sum of the synthesized output voltages of series connected sine-modulation full bridge inverters and 'V_{rec}' is the phase-shifted AC voltage of high-frequency bi-directional rectifier regarding to the square wave, *square(t)*. And the inductance between two voltage sources is the summation of the leakage inductance of high frequency transformers and additional inductance if needed. If the fundamental component of sine-modulated voltage and phase-shifted voltage, which are the components at the switching frequency of sine-modulated inverter, can be given as (8), then the transferred power between two high frequency voltage sources can be derived as (9).

$$V_{send\_fund} = V_{s1}[\cos(2\pi f_c) + j\sin(2\pi f_c)]$$
$$V_{rec\_fund} = V_{r1}[\cos(2\pi f_c + \phi) + j\sin(2\pi f_c + \phi)] \quad (8)$$

where 'ϕ' is the phase-shifted angle.

$$P = \frac{V_{s1}V_{r1}}{2X}\sin\phi \quad (9)$$

where 'X' is the impedance of the sum of the leakage inductances.

Hence, the allowable maximum magnitude of phase-shift angle is given as $\frac{\pi}{2}$.

The phase-shift can be used for the 2nd DC-link voltage control. Fig. 6 shows a block diagram of phase-shift angle controller for the power transfer via the high-frequency link. In Fig. 6, 'V_o'and 'V_o^*' stand for the DC-link voltage of high-frequency bi-directional rectifier and its reference respectively. If the reference DC-link voltage at DC source/load side, that is the 2nd DC link, is given, then a Proportional and Integral (PI) controller adjust the phase-shift angle to regulate the DC-link voltage. The output of PI controller is the reference power and the power is changed to corresponding phase shift angle according to (9).

Fig. 7 demonstrates the voltage synthesizing of sine-modulated full bridge inverter and high-frequency bi-directional rectifier at powering mode operation. In Fig. 7, the solid black triangle is the triangular carrier of sine-modulated full bridge inverter and the red dotted one is that of high-frequency bi-directional rectifier. As shown in the figure, the carrier of sine-modulated full bridge inverter leads that of high-frequency bi-directional rectifier by 90 degree because of the magnitude of allowable maximum phase-shift angle.

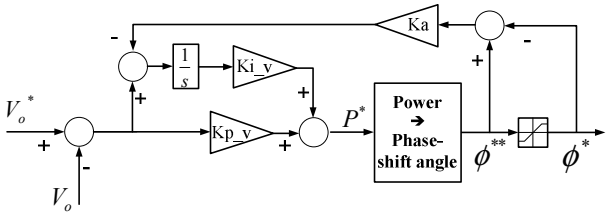

Fig. 6. Block diagram of phase-shift angle controller

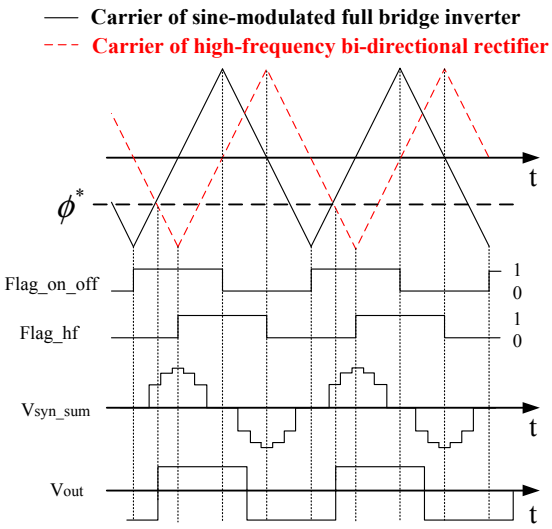

Fig. 7. Voltage synthesize of sine-modulated full bridge inverter and high-frequency bi-directional rectifier

When the phase-shift angle reference meets the falling instant of triangular carrier of high-frequency bi-directional rectifier, the positive output voltage of high-frequency bi-directional rectifier is generated during a half of switching period and the negative voltage is generated during next half period. Then, if the phase-shift angle reference is zero, the output voltages of sine-modulated full bridge inverters and high-frequency bi-directional rectifier are in phase and there is no power transfer. The larger the phase-shift angle is, the more power can be transferred.

E. Power factor control

Fig. 8 shows the simplified single phase equivalent circuit of SUL converter. In Fig.8, 'E_a' and 'i_a' is the input phase voltage and current, 'L_s' is the source inductance, 'L_F', 'R_F', 'C_F' is the input filter inductance, damping resistor, and capacitance, and 'C_{dc}' is the 1st DC-link capacitor respectively. Also, the load current is modeled as a current source, 'i_{a_h}'.

If the capacitor voltage, 'V_c', and load current are in phase and only their fundamental components are considered, the following equation can be derived.

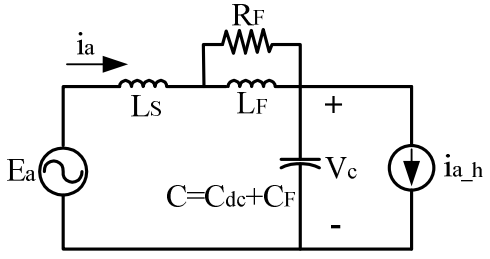

Fig. 8. Simplified single phase equivalent circuit of SUL converter

$$
\begin{aligned}
i_a &= C\frac{dV_c}{dt} + i_{a\_h} \\
&= \sqrt{(CV\omega)^2 + I^2}\,\sin(\omega t + \psi) \\
\psi &= \tan^{-1}\left(\frac{CV\omega}{I}\right)
\end{aligned} \tag{12}
$$

where $V_c = V\sin(\omega t)$ and $i_{a\_h} = I\sin(\omega t)$.

The input displacement factor may be poor at the low load current because of the large capacitance.

Usually, the grid-connected power converter can control the input power factor by PWM of input grid side converter. However, the switching instant of low-frequency bi-directional rectifier of SUL converter is fixed by the input phase voltage and there is no degree of freedom to control the input power factor. In order to control the input power factor, SUL converter modifies the synthesized voltages of sine-modulated full bridge inverter. The sine-modulated voltage of (3) can be modified using the switching function of low-frequency bi-directional rectifier as follows,

$$
\begin{aligned}
&V_{ac\_a} \\
&= mV_{dc\_a}\,sign(\sin(\omega t))\sin(\omega t + \varphi)square(t) \\
&V_{ac\_b} \\
&= mV_{dc\_b}\,sign\left(\sin\left(\omega t - \frac{2}{3}\pi\right)\right)\sin\left(\omega t - \frac{2}{3}\pi + \varphi\right)square(t) \\
&V_{ac\_c} \\
&= mV_{dc\_c}\,sign\left(\sin\left(\omega t + \frac{2}{3}\pi\right)\right)\sin\left(\omega t + \frac{2}{3}\pi + \varphi\right)square(t)
\end{aligned} \tag{11}
$$

where 'φ' is the desired phase angle between the input phase voltage and current.

Using (11), the series-connected output voltage of sine-modulated full bridge inverter can be derived as (12).

$$
\begin{aligned}
V_{syn\_sum} &= n\left(V_{ac\_a} + V_{ac\_b} + V_{ac\_c}\right) \\
&= \frac{3}{2}nmV\cos(\varphi)square(t)
\end{aligned} \tag{12}
$$

By the power balance at 1st DC-link and the switching function of low-frequency bi-directional rectifier, the input phase currents can be derived as follows,

$$
\begin{aligned}
i_a &= i_{out\_a}\sin(\omega t + \varphi) \\
i_b &= i_{out\_b}\sin\left(\omega t - \frac{2}{3}\pi + \varphi\right) \\
i_c &= i_{out\_c}\sin\left(\omega t + \frac{2}{3}\pi + \varphi\right)
\end{aligned} \tag{13}
$$

III. Experimental Results

Fig. 9 is the photo of an experimental AC/DC power converter for feasibility test and Table.1 shows the parameters of the converter. The input phase r.m.s. voltage is 220 V, the switching frequency of sine-modulated full bridge inverter and high-frequency bi-directional rectifier is set as 15 kHz and three 4 kVA high-frequency transformers are installed. Fig. 10 shows the photo of high-frequency transformer and Table.2 demonstrates the parameters of high-frequency transformer.

To do the experiment, the resistor is connected at 2nd DC-link capacitor in powering mode and the DC-power supply with current control mode is connected in regenerating mode.

The reference of 2nd DC-link voltage at DC source/load side is set to 180 V in order to have the same voltage rating of all H-bridge modules.

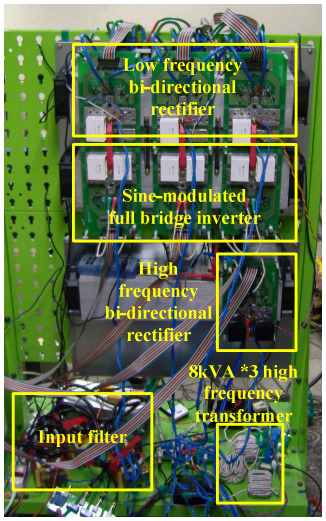

Fig. 9. Photo of the proposed AC/DC power converter

TABLE I
PARAMETERS OF THE PROPOSED AC/DC POWER CONVERTER

quantity	Value
Input phase r.m.s. voltage	220V 60Hz
Input filter parameters	L_F ; 100μH C_F ; 47μF R_F ; 3Ω
1st DC-link capacitance	12μF
2nd DC-link capacitance	94μF
Switching frequency of high frequency power transfer	15kHz

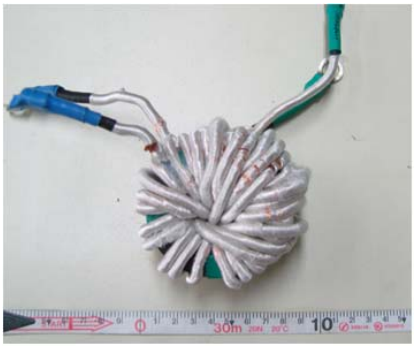

Fig. 10. Photo of 4kVA high-frequency transformer

TABLE II
PARAMETERS OF HIGH-FREQUENCY TRANSFORMER

quantity	Value
Capacity	8 kVA
Rated voltage	Primary ; 180V Secondary ; 120V
Rated current	Primary ; 44A Secondary ; 67A
Turn ratio	3 : 2
Core material	Finemet

Fig. 11 shows the output voltage of 'a' phase sine-modulated full bridge inverter according to 1st DC-link voltage. As shown, the DC-link voltage is the rectified version of the input AC phase voltage. The output voltage of sine-modulated full bridge inverter has positive and negative value during a switching period and its average is zero. Fig. 11 (b) is the expansion of red-dotted rectangular part in Fig. 11 (a). As the magnitude of 1st DC-link voltage is increased, the magnitude and the width of the synthesized voltage are increased because of the sine-modulation.

Fig. 12 shows the input 'a' phase current and voltage at the 4 kW powering and 3.6 kW regenerating operation. The input AC current to grid is sinusoidal and the phase of input current is decided by the operating mode. Also, Fig. 13 depicts the FFT results of input current of Fig. 12. As shown in the figures, the input current to grid is sinusoidal and all harmonics are below 3 % compared to the fundamental component.

Fig. 14 demonstrates the input power factor control at 3.2 kW powering operation. Fig. 14 (a) is the waveforms when the desired phase angle is zero and Fig. 14 (b) is those when it is -25 degree. As mentioned in Section II-E, when the desired phase angle is zero, the input 'a' phase current is leading to input 'a' phase voltage due to the filter capacitance. However, as the desired phase angle is lagging, the input power factor can be modified.

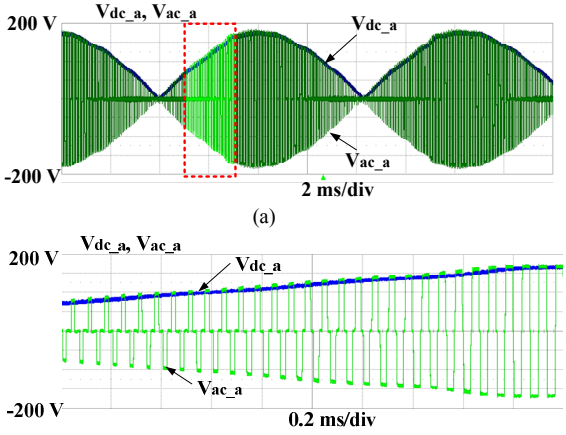

(b) Expansion version of (a)

Fig. 11. 1st DC-link voltage and output voltage of 'a' phase sine-modulated full bridge inverter

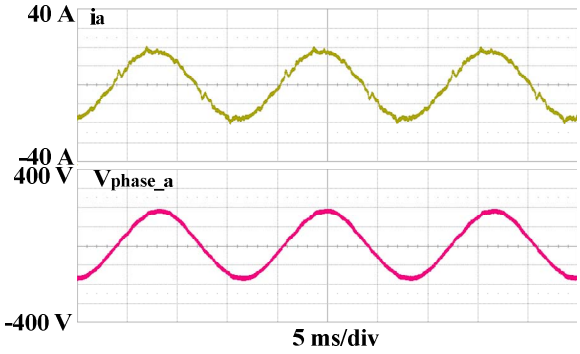

(a) 4 kW powering operation

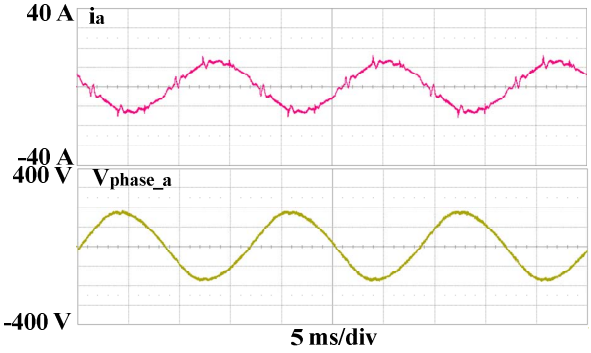

(b) 3.6 kW regenerating operation

Fig. 12. 'a' phase input current and voltage

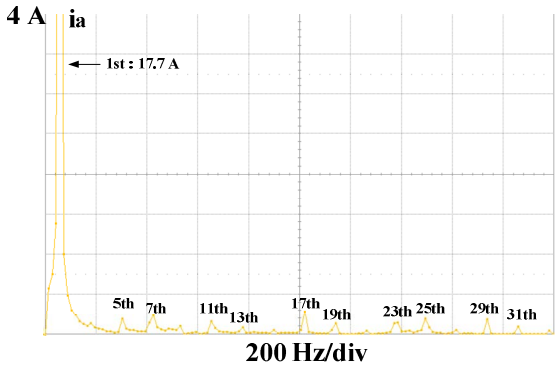

(a) 4 kW powering operation

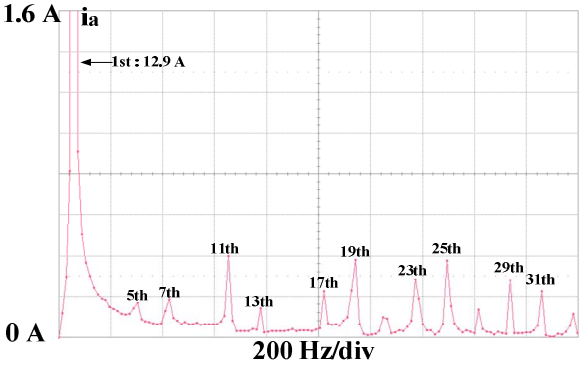

(b) 3.6 kW regenerating operation

Fig. 13. FFT results of 'a' phase input of Fig. 12

Fig. 15 demonstrates the input power factor control at 2.7 kW regenerating operation. Fig. 15 (a) is the waveforms when the desired phase angle is zero and Fig. 15 (b) is those when it is 25 degree. Like a motoring mode operation, when the desired phase angle is zero, the input 'a' phase current is lagging to input 'a' phase voltage. As the desired phase angle is changed, the input power factor is also changed.

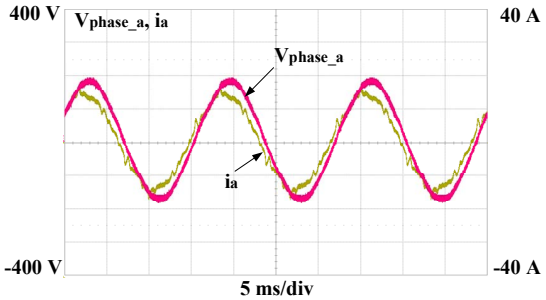

(a) phase angle : zero

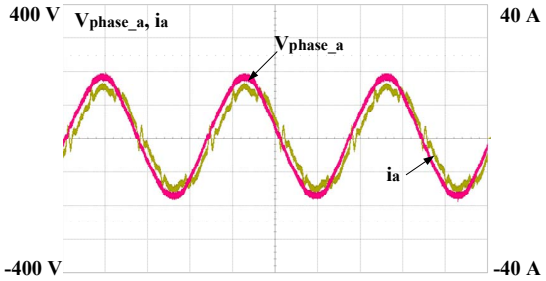

(b) phase angle : 25 degree lagging

Fig. 14. Power factor control at 3.2 kW powering operation

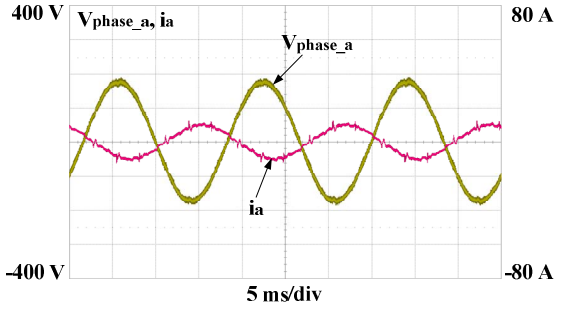

(a) phase angle : zero

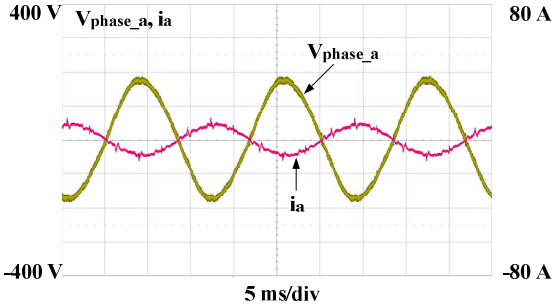

(b) phase angle : 25 degree leading

Fig. 15. Power factor control at 2.7 kW regenerating operation

IV. Conclusions

In this paper, a novel AC/DC power converter is presented. The proposed Series-connected Universal Link (SUL) converter has many attractive features as follows,

- Reduced reactive components
- Sinusoidal input AC current
- Compact and modular construction
- Capability of bi-directional power flow
- Capability of power factor control
- Galvanic isolation and flexibility of the voltages with high frequency transformer

Consequently, SUL converter can satisfy the needs of the future electric energy conversion and it might be a backbone to Smart Grid to accommodate various renewable energy sources and energy storage system.

References

[1] B. Gemmell, J.Dorn, D.Retzmann, and D. Soerangr, "Prospects of Multilevel VSC Technologies for Power Transmission," in *Proc. IEEE-Power Engineering Society Transmission and Distribution Conf.*, pp. 1-16, 2008.

[2] M.Cacciato, A.Consoli, R.Attanasio, and F. Gennaro, "Soft-Switching Converter With HF Transformer for Grid-Connected Photovoltaic Systems," *IEEE Trans. Industrial Electronics*, vol. 57, pp. 1678-1686, May. 2010.

[3] Z.Chen, J.M.Guerrero, and F.Blaabjerg, "A Review of the State of the Art of Power Electronics for Wind Turbines," *IEEE Trans. Power Electronics*, vol. 24, pp. 1859-1875, Aug. 2009.

[4] S.K.Sul, Electric Machine Control Theory, 2nd ed. Seoul, Korea : Hongneung Science, 2007.

[5] J.Jung, S.Lim, and K.Nam, "A Feedback Linearizing Control Scheme for a PWM Converter-Inverter Having a Very Small DC-link Capacitor," *IEEE Trans. Industry Applications*, vol. 35, pp. 1124-1131, Sep/Oct, 1999.

[6] L.Malesani, L.Rossetto, P.Tenti, and P.Tomasin, "AC/DC/AC PWM Converter with Reduced Energy Stroage in the DC Link," *IEEE Trans. Industry Applications*, vol. 31, pp. 287-292, Mar/Apr, 1995.

[7] S.Kim, S.K.Sul, and T.A.Lipo, "AC/AC Power Conversion Based on Matrix Converter Topology with Unidirectional Switches," *IEEE Trans. Industry Applications*, vol. 36, pp. 139-145, 2000.

[8] A.Yoo, W.J.Lee, S.Kim, B.M.Dehkordi, and S.K.Sul, "Input Filter Analysis and Resonance Suppression Control for Electrolytic Capacitor-less Inverter," in *Proc. IEEE Applied Power Electronics Conf.*, pp. 1786-1792, 2009.

[9] R.De Doncker, D.M.Divan and M.H.Kheraluwala, "A Three-Phase Soft-Switched High-Power-Density dc/dc Converter for High-Power Applications," *IEEE Trans. Industry Applications*, vol. 27, pp. 63-73, 1991.

[10] S. Inoue, and H.Akagi, "A Bidirectional Isolated DC-DC Converter as a Core Circuit of the Next-Generation Medium-Voltage Power Conversion System," *IEEE Trans. Power Electronics*, vol. 22, pp. 535-542, 2007.

[11] A.J.Watson, HQS Dang, G.Mondal, J.C.Clare, and P.W.Wheeler, "Experimental Implementation of a Multilevel converter for power system integration," in *Proc. IEEE Energy Conversion Congress and Exposition Conf.*, pp. 2232-2238, 2009.